D1: Report describing the new reference fields for dosimetry in electron beams with ultra-high pulse dose rates.

Project:	18HLT04 UHDpulse
Lead partner:	PTB
Deliverable due on:	Aug. 2021
Submission date:	November 2021

Contents

1. Introduction

The objective of work package WP1 of the project entitled "Metrology for advanced radiotherapy using particle beams with ultra-high pulse dose rates" funded by the European Metrology Program for Innovation and Research (EMPIR) was to provide the metrological input needed to support absolute dosimetry of particle beams with Ultra-High Pulse Dose Rate (UHPDR), generated with conventional and novel laser-driven accelerators. Task 1.1 will lead to the establishment of the reference radiation fields for electron beams with ultra-high dose per pulse enabling traceable calibrations of detectors for this radiation modality. This report on reference fields with ultra-high dose per pulse electrons is based on the investigations made within this work package and more specifically, the task A 1.1.2, A 1.1.3 and A1.1.4. This report is the deliverable No. 1 according to the JRP protocol.

The following partners contributed to this deliverable:

- Physikalisch-Technische Bundesanstalt (PTB)
- Eidgenössisches Institut für Metrologie (METAS)
- Główny Urząd Miar (GUM)

In section 2 of this report, the PTB facility, equipment, reference electron beam characteristic and monitoring will be presented. In section 3, the METAS facility, equipment, reference beam characteristic will be presented.

2. PTB - UHPDR reference electron beam

This section will present the reference UHPDR electron beam optimised at the Electron accelerator facility for radiotherapy dosimetry at PTB-Braunschweig, Germany. The following subsection 2.1 will cover information about the linear research accelerator at PTB and available equipment. The work presented in the following subsection 2.2 and 2.3 are the results of measurement and Monte Carlo simulation carried between December 2020 and March 2021. The resulting optimisation and characterisation of the PTB UHPDR electron beam was used for an experimental measurement related to the UHPDR project in spring 2021 (activity A2.1.5). The beam was closely monitored throughout the experiment and the resulting absolute calibration, stability and monitoring will be presented in section 2.5 and 2.4.

2.1. PTB research linear accelerator facility

The PTB's 11-meter-long accelerator for fundamental dosimetry research is a custom-built linear accelerator (linac). The linac can accelerate electrons for production of pulsed electron beams of monoenergetic energies between 0.5 to 50 MeV. The beam properties: position, profile, spectral electron fluence or the beam current can be measured using dedicated equipment. The following sections will present some characteristics of linear accelerators and the equipment used in the aim to characterise the in-vacuum electron beam.

The research linear accelerator at the PTB-Braunschweig facility consists of 2 sections: a low- and a high-energy section. This document will only present and focus on the high-energy section as it is the one that has been optimized for the UHPDR reference electron beam. For this project, the beamline (Figure 1) has been optimized to reach UHPDR with a beam with an average energy of 20 MeV. This energy has been selected to provide more flexibility for dosimetry as the reference depth is a few centimetres in water, but still been clinically relevant. The research accelerator details can be found in the following document: The Metrological Electron Accelerator Facility (MELAF) for Research in Dosimetry for Radiotherapy (DOI:10.1007/978-981-10-9023-3_109) [1].

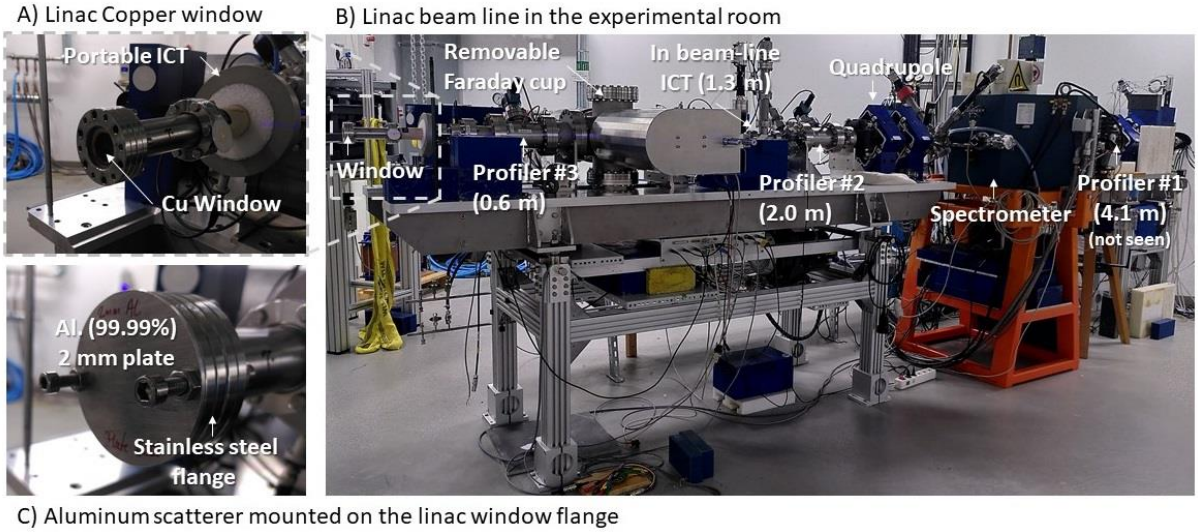

Figure 1: Picture of the high energy beamline of the PTB research electron accelerator and close-up picture of the Cu beam exit window and scatterer. A) Close-up picture of the 100 µm Cu exit window and the portable ICT (secondary monitoring). B) Picture of the beamline. The distances indicated are up to the end beamline exit window. C) Close-up picture of an aluminium plate, used as scatterer, mounted on the exit window flange.

The in-vacuum electron beam has been characterized in terms of shape, energy, and time structure. The electron beam energy has been measured using a magnet spectrometer (Figure 1 B). The beam spatial shape was measured using two wire scanners (labelled as Profiler #2 and #3 in Figure 1 B). The beamline is equipped with an insertable Faraday cup and two Integrating Current Transformers [2], a fixed (in-flange) ICT and a portable ICT which is positioned closer to the linac window as illustrated in Figure 1 B). The fixed ICT is a Bergoz ICT (in-flange version, turns ratio 50:1, ICT-CF4.5/34.9-070-50:1-UHV, SN 1650) is used as monitor for dosimetry and to determine the absorbed dose to water after its calibration against alanine. The in-house built portable ICT is used to optimise linac gun and RF power, but also as a back-up system.

The temporal structure of the electron beam is measured using an in-house built ICT connected to an oscilloscope. The beam pulse repetition frequency (PRF) is 5 Hz and the pulse width is 2.5 µs as illustrated in Figure 2. The research linac is equipped with a slit of adjustable position that is located downstream from the bending magnet for separation of a monoenergetic beam at the end of the linac. These so-called energy slits (ES) can be used to vary the electron fluence which directly impacts the dose-per-pulse, while minimally influencing the beam characteristics, trajectory, shape, and energy. The width of the energy slit is changed between fully open to close position (specified in mm). The electron beam exits the linac vacuum pipe through a 100 µm copper window. In addition to the beam exit window, metal plates can be mounted on the exit flange to provide more scattering, see Figure 1 C).

Figure 2: Instantaneous current of a pulse delivered by the research linear accelerator measured with an Integrating Current Transformer (ICT) connected to an oscilloscope. The pulsed charged measured is 250 nC.

The absolute and relative dosimetric measurements have been performed in a water phantom installed on a translation table as illustrated in Figure 3. The distance between the outer wall surface of the water tank facing the linac and the linac exit window, the source-to-surface distance (SSD), was measured using a laser range finder (± 3.0 mm, Bosch, Gerlingen Germany). The water tanks used at PTB are usually made of PMMA, however, PMMA has shown to accumulate radiation damage quickly in the context of UHPDR electron beam. Consequently, the water tank which has a dimension of 30×30×30 cm^3, consists of 1 cm thick PMMA walls except the entrance window which is a 0.776 cm thick clear polycarbonate plate. The polycarbonate has shown to be less radiation sensitive, however, it quickly turns to a dark opaque brown, therefore, the clear PMMA side wall was useful for dosimeter positioning. The water tank is equipped with a motorized precise XYZ positioning system to position the dosimeter and can be adapted to accommodate different detectors.

The absolute dosimetry has been done by means of Alanine which will be presented in detail in subsection 2.5. The relative dosimetry has been performed using a diamond detector prototype, B1, which has shown linearity for a large range of dose-per-pulse (REF Marinelli).

The diamond detector is a highly conductive p-type structure. The sensitive volume of the detector is a diamond of density 3.53 g·cm-3 with an active volume of 1.0 µm thick and a radius 0.7 mm side. The diamond detector prototype is waterproof and has an equivalent water thickness of 1 mm upstream of the sensitive volume. The biggest advantages of using diamond for relative measurement are; a small sensitive volume in directions orthogonal and parallel to the beam axis, the capability for real-time measurements and a stopping power ratio water to diamond which can be assumed as constant in good approximation for the energy range investigated here.

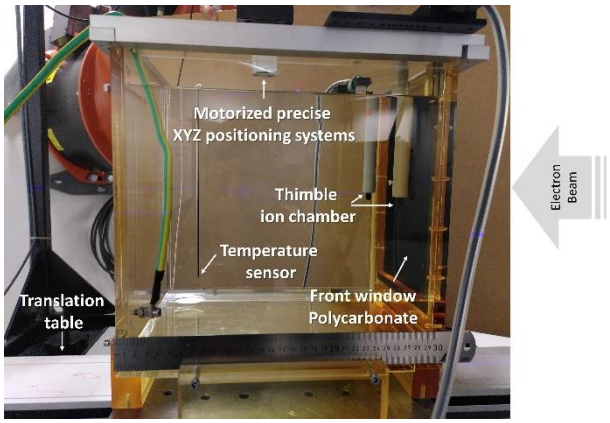

Figure 3: Picture of the water tank used during the measurement at the PTB research accelerator in UHPDR mode.

In addition to experimental measurements, Monte Carlo models of the linac have been developed at PTB using `EGSnrc` software toolkit [3], release v2020, and a `FLUKA` [4] model was developed at GUM. These models have been developed independently. PTB has provided to GUM the in-vacuum beam characterization parameters which will be presented below, and the geometric description of the beamline (Figure 1). At GUM, a depth dose curve and lateral dose profiles in horizontal and vertical direction at the reference depth in a water cube of 30 cm sides was simulated. The Monte Carlo models have been compared to each other and to the experimental relative measurements in water. The `EGSnrc` model has been used to simulate and optimize the electron reference beam to reach a variety of dose-per-pulse ranges and beam shapes and sizes.

2.2. UHPDR electron beam characteristics in linac beamline

In this section, the in-vacuum characterisation of the electron beam shape and energy spectrum will be presented. The beam line has been optimised to deliver a 20 MeV electron beam in UHPDR pulse mode. The energy spectrum has been measured by a magnet spectrometer and the results of the measurement are shown in Figure 4. The measurement has been performed for the highest possible fluence, i.e., when the energy slits are fully open. The measured energy spectrum was simplified as a gaussian shape for the Monte Carlo simulation. From these measurements, it was decided to model the source as a gaussian type with a mean energy of 20.006 MeV and a sigma of 0.047 MeV for all ES positions.

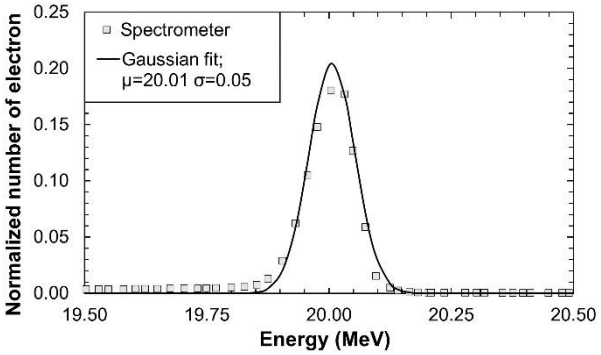

Figure 4: Energy spectrum of the high-energy electron beam optimised for the PTB research in UHPDR pulse mode. The squares are the measured value normalized and the line is the best fit gaussian.

The electron beam profile in-vacuum has been measured using wire scanners (profiler) that are the closest to the exit window; number 2 and 3 as illustrated in Figure 1. The beam profile measurement has been done for ES lateral positions between 0 to 10 mm by steps of 1 mm and for a fully open position (about 24 mm). The measurements and `EGSnrc` beam profile in-vacuum are shown in Figure 5. For clarity purposes, only the results for ES position 2, 6 and 10 mm are shown. The black solid lines are the measurements at the profiler 2 (2.0 m upstream from the exit window), the coloured solid lines are the measurements at the profiler 3 (0.6 m upstream from the exit window), and the dashed and doted lines are the in-vacuum beam profile generated by Monte Carlo simulation at the window position and at the position of profiler 3, respectively. The beam size, FWHM, of the beam are listed in Table 1.

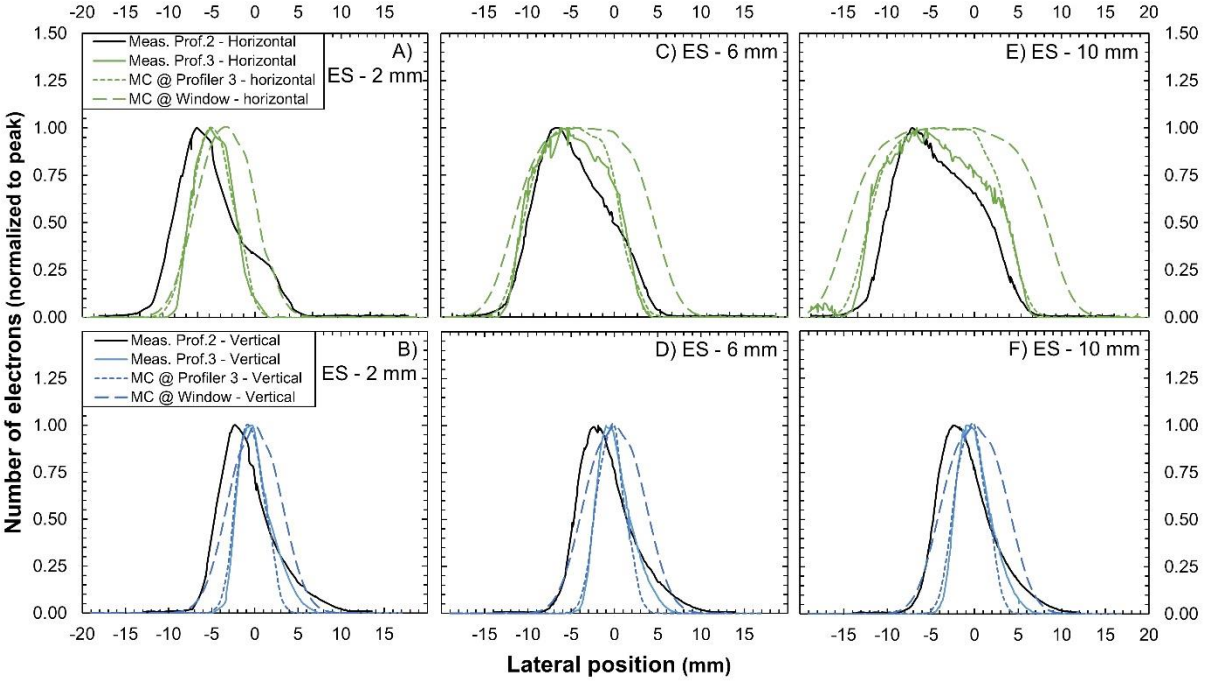

Figure 5: The in-vacuum electron beam profile measured and simulated. The upper panels represent the horizontal profile measurements, and the lower panels represent the vertical profile measurements for different ES position; A) and B) 2mm, C) and D) 6 mm and E) and F) 10 mm position.

Table 1: Dimension of the electron beam in the vacuum beamline of the PTB research accelerator.

Energy slits position	Vertical axis Dimension and position (mm)		Horizontal axis Dimension and position (mm)	
	Profiler #2	Profiler #3	Profiler #2	Profiler #3
	FWHM	FWHM	FWHM	FWHM
ES - 02	6.0	4.1	5.5	4.3
ES - 06	6.2	4.4	7.6	9.0
ES - 10	6.2	4.2	9.7	13.0

As illustrated in Figure 5, the vertical beam profiles measured for different settings of the energy slits are very similar while the horizontal profiles are changing significantly as illustrated in the top panels. This observation was expected as the ES are metal plates moving and blocking the beam in the horizontal direction. The in-vacuum beam size is larger at the profiler #2 compared to the one measured at the profiler #3, except for the 6 and 10 mm ES position in horizontal axis (Figure 5 E)). It was therefore decided to simulate the point source position between the two profilers according to the measured dimension. This is explained schematically in Figure 6.The target shape is an ellipse defined at the position (0,0,0) to reproduce the different beam shapes measured depending on the ES position. A gaussian spread was applied to the beam to obtain a non-uniform fluence throughout the target shape as illustrated in Figure 5. In the `EGSnrc` simulation, the geometry only starts at the exit window (defined at the position (0,0,0)), therefore, the linac vacuum pipes are not simulated. The trajectory of simulated electrons is therefore linear from the initial point source shape to the targeted ellipse shape, electron interaction with matter starting at the exit window.

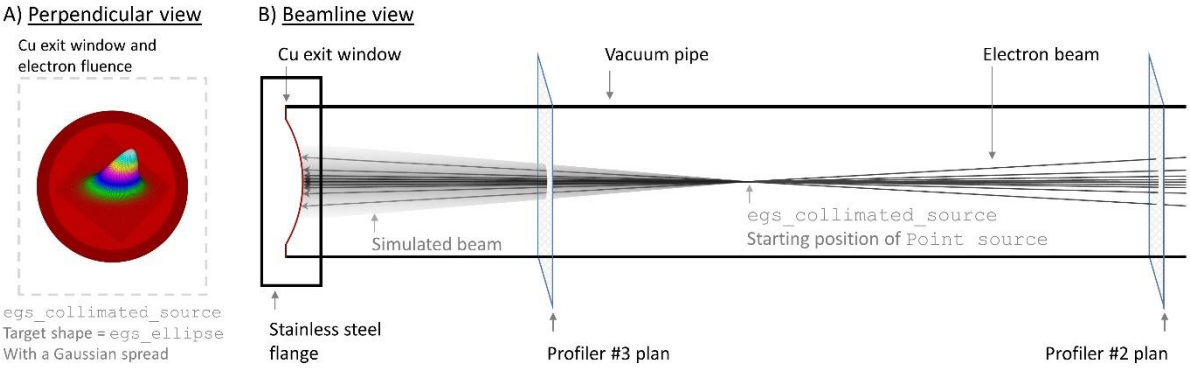

Figure 6: Schema of the linac vacuum beamline and the electron beam profile with an overlaid representation of the source simulated by Monte Carlo.

2.3. UHPDR electron beam characteristics in water

The electron beams will be characterized in terms of beam size, beam quality specifier (Q) and the depth of 95% dose (R_{95}). The beam size is defined as the full width at half maximum (FWHM), i.e., the distance between the points at which the dose amounts to 50% of the maximum dose in horizontal and vertical directions perpendicular to the beam direction. The beam quality specifier in UHPDR electron beam is the same as defined in conventional dose rate code of practice, R_{50}, which is the depth on the beam axis where the absorbed dose is equal to 50% of the maximum dose. Accordingly, the depth of 95% dose, R_{95}, is the depth where the absorbed dose is equal to 95% of the maximum dose. The reference depth for absorbed dose measurements, z_{ref}, is also defined as in conventional dose rate code of practice [5], [6] as:

$$z_{ref} = 0.6 \cdot R_{50} - 0.1 \text{ cm} \qquad \text{Eq. 1}$$

2.3.1. Beam set-up investigated

In the aim to test the EGSnrc beam model presented in Figure 5 and Figure 6, measurement of depth dose curves and beam profiles has been carried out at the SSD of 70 cm using the diamond detector prototype. The beam quality specifier (R_{50}), the profile flatness within 3.0 cm diameter and the FWHM of profiles at the depth of z_{ref} obtained with EGSnrc and FLUKA simulation are compared to the results obtained using the diamond detector prototype and listed in Table 2. The difference in the beam quality specifier obtained are less than 1 mm between the simulation and measurement.

Table 2: Dimension of the electron beam in the vacuum beamline of the PTB research accelerator.

	EGSnrc	FLUKA	Measurement
R_{50} (cm)	7.92	7.80	7.87
Flatness at z_{ref}	9.3%	8.9%	9.7%
FWHM at z_{ref} (cm)	8.2	8.04	8.04

The EGSnrc model has been used to investigate a total of seven different possible set-up to enable different dose rate range and beam size in water by using simple scatterer plate, flattening filter (FF) and a cylindrical PVC tube for collimation. The list of the set-up investigated can be found in Table 3. A preliminary reference electron beam with an SSD of 70 cm was calibrated by means of alanine measurement. The calibration provided baseline information to predict absolute dose-per-pulse range for each set-up investigated.

The collimation system investigated was a 500 mm long PVC tube and is illustrated in Figure 7. A plastic tube shape was selected for the simplicity of the design and the light weight which make it practical for installation. The material, PVC, was selected for its low price, availability and it was possible to buy with an inner diameter of 50 mm which was the targeted beam shape. The scatterers, 1 or 2 mm thick, are uniform plate made of 99.99% pure aluminium. This material was selected for its availability, easily machinable and it is a low atomic number which is convenient for radioprotection. The scatterer, when used, has been mounted to the linac exit window stainless steel flange to ensure a perpendicular intersection of the electron beam, shown in Figure 1. The flange provided a reproducible distance of 7.6 mm between the copper exit window and the plate.

Table 3: List and description of the different electron beam set-ups investigated by Monte Carlo simulation.

Set-up name	SSD (cm)	Collimation	Scatterer and Flattening filter
SSD50-00	50	None	None
SSD50-00c	50	PVC tube	None
SSD50-01c	50	PVC tube	Al. 1 mm plate
SSD50-02c	50	PVC tube	Al. 1 mm plate + FF
SSD70-00	70	None	None
SSD90-00	90	None	None
SSD90-02	90	None	Al. 2 mm plate

A flattening filter was designed and optimized to reach a flatness better than 5% over a diameter of 30 mm at the depth of the R_{95}. Multiple flattening filter designs were generated using a dedicated simulation program, Dual Foil Simulator [7], and each design was tested using Monte Carlo simulation. The final design selected was a 2 mm thick filter with a gaussian

shape made of 4 segments of uniform thickness (0.5 mm). The radius of each segment was 5, 8, 12 and 25 mm respectively. The flattening filter is illustrated in Figure 7 C).

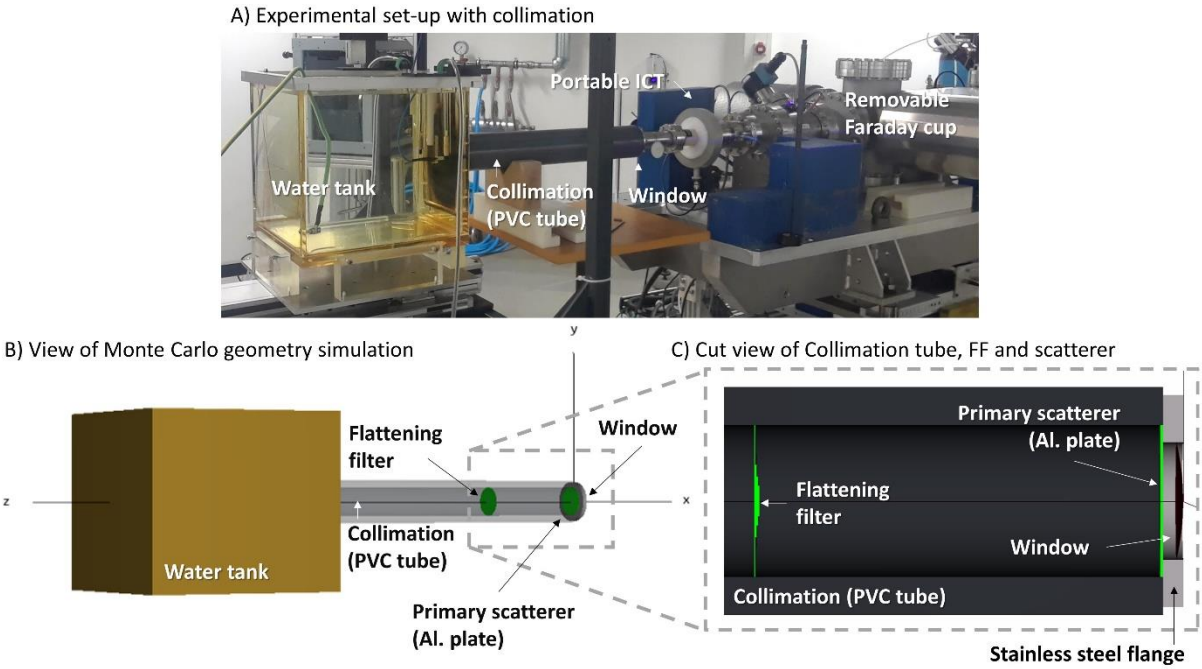

Figure 7: Illustration of the experimental set-up SSD50-02c. The flattening filter is positioned at 15 cm from the exit window. A) Picture of the experimental set-up, B) View of the Monte Carlo simulation representing the set-up in A) and C) zoom of a cut view of B) to show the shape of the flattening filter.

The results of the measurement compared to Monte Carlo are shown in Figure 8. The simulated beam characteristics are given in Table 10 which can be found at the end of this document. The difference between the beam characteristic measured and simulated are found in brackets in Table 10.

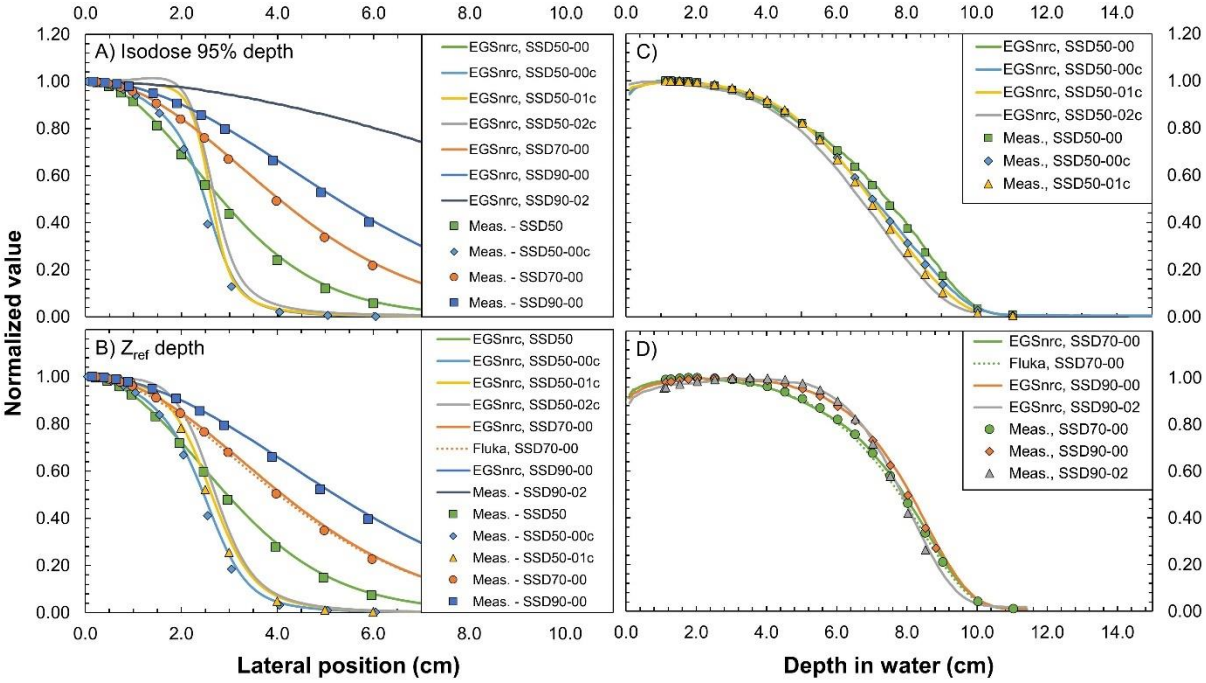

Figure 8: Simulated and measured profiles and depth dose curves. A) and B) are the profile at depth of R_{95} and at the reference depth, z_{ref}. Due to symmetry – only half of the

profiles are shown. C) and D) show the depth dose curves which have been separated into two panels for clarity.

From the EGSnrc simulation and measurement results shown in Figure 8, it was decided to use the beam set-up SSD70-00 and SSD90-02 as the reference beam for UHPDR electron beam at PTB. The use of two set-ups enables a wide range of dose-per-pulse, between 0.13 to 6.7 Gy-per-pulse. The two set-ups are also very simple and quick to install. Beams using collimation were not selected as UHPDR electron beam reference at PTB since the positioning of the PVC tube was time consuming. Its installation required multiple iterations of profile measurement and repositioning to ensure that the tube is well aligned with the electron beam. It is possible to install a single collimated beam set-up for longer-term use, however, a smaller range of doses-per-pulse are achievable.

The flatness of the set-up SSD90-02 was reaching the goal of ± 3% flatness level at the depth of R_{95} and in the context of PTB research, collimation is not required. Another important advantage was the very similar reference depth for both beams, 46.5 and 46.2 mm for the beam set-up SSD70-00 and SSD90-02 respectively. Although the mean energy of the beam is smaller for the set-up SSD90-02 as listed in Table 10 and shown in Figure 10, the beam size also impacts the depth of R_{50} and thus z_{ref}. From the simulation, it was decided to establish the reference depth at 46.5 cm in water for both beams.

The influence of radial non-uniformities of the beam profile was studied for both selected reference electron beams for a range of sensitive (scoring) volume radius. The results of the simulated and measured values are shown in Figure 9 along with a quadratic fit. The correction factor is estimated to be smaller than 1.0010(10) for sensitive volume with radius in the orthogonal direction smaller than 1.6 and 5.0 mm for the set-up SSD70-00 and SSD90-02 respectively.

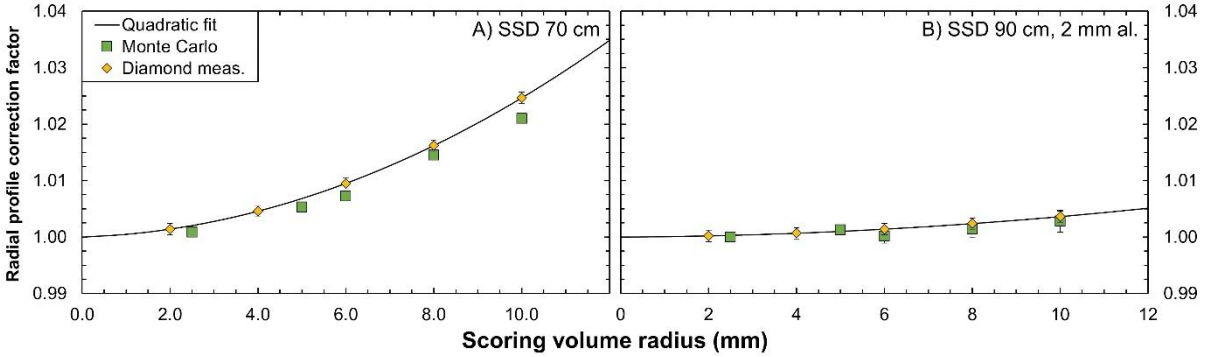

Figure 9: Correction factor for the lateral variation of the beam intensity.

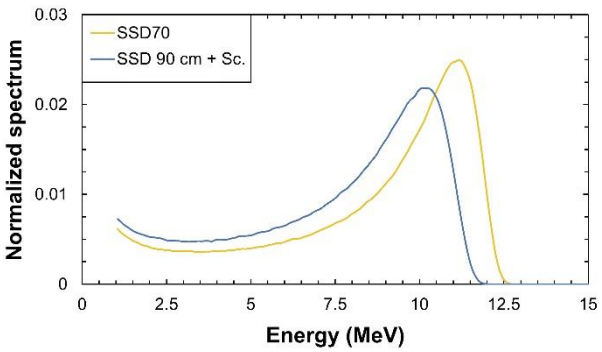

Figure 10: Energy spectrum at the depth of 46.5 mm for the reference UHPDR electron beam simulated by Monte Carlo EGSnrc using cavity application.

As shown in Figure 5, the in-vacuum beam profile size can change significantly with the ES slit width selected. To investigate the impact of the beam size at the beam exit window on the dose in water, the beam profile in water at z_{ref} was simulated using Monte Carlo and compared to measurement using the diamond detector prototype B1 for the initial reference beam, SSD70-00. The resulting characterisation is shown in Table 4.

Table 4: Characterisation of the energy slit width impact on the horizontal beam size and relative dose deposited at the reference point of measurement.

		FWHM horizontal (*mm*)		Normalized signal to ES - 2 mm	
ES width	z_{ref} (*mm*)	MC	Meas.	MC (±0.6%)	Meas. (±0.3%)
Close	46.6	81.9	80.0	1.0090	1.0001
2 mm	46.6	82.4	80.2	1	1
4 mm	46.6	82.5	80.4	0.9944	0.9920
6 mm	46.7	82.6	81.1	0.9884	0.9812
8 mm	46.6	83.7	81.8	0.9684	0.9674
10 mm	46.7	84.5	82.1	0.9557	0.9641
Open	46.7	84.0	82.4	0.9602	0.9584

As shown in Table 4, the change in the ES changes the beam size in water at z_{ref} by more than 2 mm, while the in-vacuum beam size change by about 10 mm. The smaller change at z_{ref} was expected due to electron scattering in water. The ES position doesn't have a significant impact on the depth of z_{ref}. However, although the beam size changed by a few millimetres, the `EGSnrc` simulation predicted a change of about 5% in the normalized signal at reference measurement point. This observation was validated by measurement with diamond detector. This will impact the relationship between the monitor signal from the in-flange ICT, and the absolute dose deposited at z_{ref} in water. It would be therefore expected to see a non-linear relationship between the in-vacuum beam fluence, and the dose deposited in water.

2.4. Beam stability and monitoring

In the spring 2021, an investigation was carried out at the PTB research linac using the reference UHPDR electron beams for 6 weeks. The stability of the linac output was also investigated. To do so, in-vacuum and in water measurements were carried out about three times a week for a total of 6 weeks. The following section will present the measurement made during the spring 2021 and will be compared with the measurement presented in the previous section; carried out in winter 2021.

2.4.1. In beam line

The in-vacuum beam profile characteristic measured is presented in Figure 11 and Figure 12. In Figure 11, the measured profile for the ES positions of 2, 6 and 10 mm of the measurement carried out in winter 2021 are compared to the measurement taken during the investigation carried out in spring 2021. In Figure 12, all the measurements are averaged over a week (3 days of measurement typically except the measurement labelled 2021-02-11 which are the measurements of that date only).

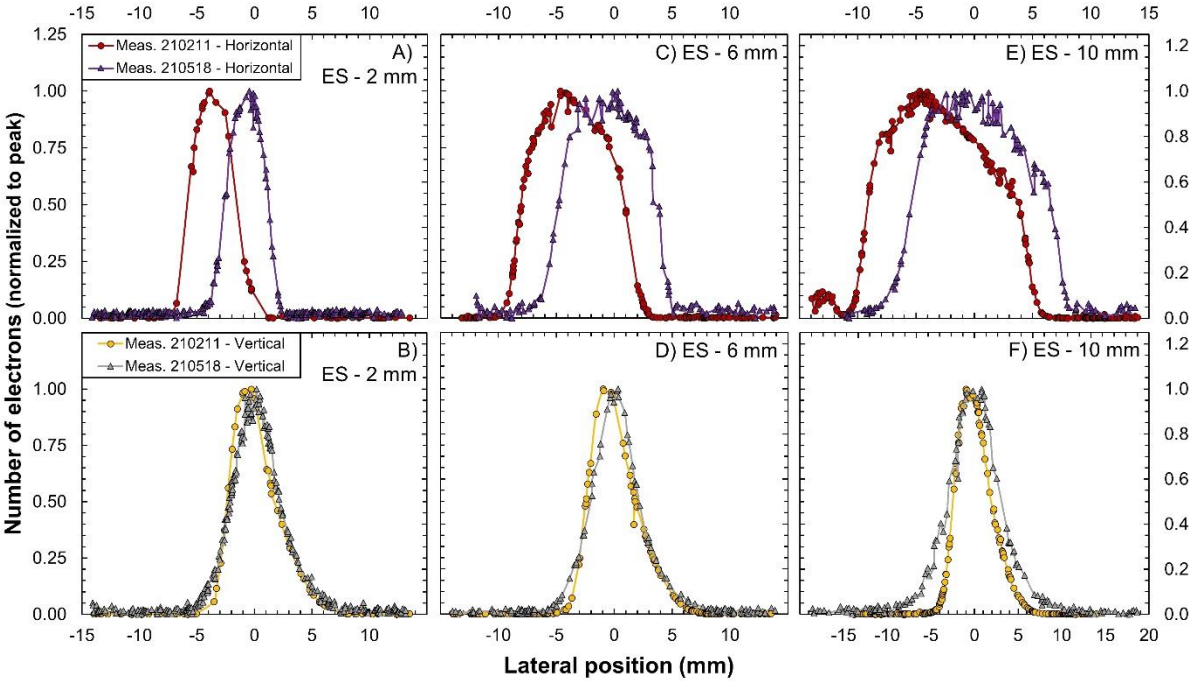

Figure 11: The electron in-vacuum beam profile measured during the investigation carried out in spring 2021, compared to the measurement carried out in winter 2021. The upper panels are the horizontal beam with the lower panels are the vertical beam profile. The panels, A) and B) are the profiles measured when the energy slits are positioned at 2 mm, C) and D); ES position 6 mm, and E) and F); ES position 10 mm.

As shown in Figure 11 and Figure 12, the only observed change of the in-vacuum beam characteristics between the measurement carried out in winter and spring 2021 is the central position of the horizontal profile. This was expected as the steerer magnet settings for central positioning of the in-vacuum beam were reoptimized to centre the beam. As shown in Figure 12, the change of this setting had a minor impact on the other beam characteristics.

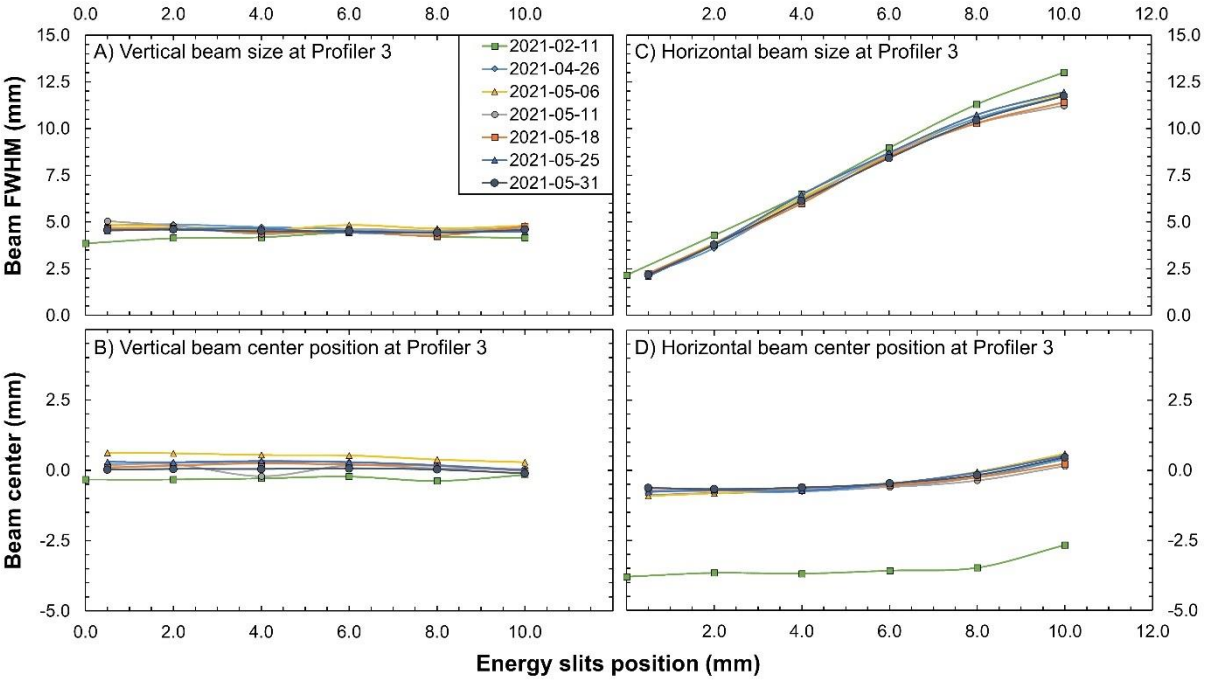

Figure 12: In-vacuum beam profile measured characteristic between winter (February) and spring 2021. The upper panels, A) and C), are the beam size (FWHM) measured and the lower panels, B) and D), are beam centre position. The left panels are

the beam profile measured in vertical direction, and the right panels in horizontal direction. The beam parameters are characterized in terms of the ES setting which are used to vary the beam fluence.

As mentioned earlier, the research accelerator is equipped with two ICT, a commercial in-flange, and a portable in-house built ICT. As the portable ICT is used as back-up system for the primary monitor, the in-flange commercial ICT, the ratio of the two ICT was monitored for further validation. The ICTs ratio from measurements between December 2020 and March 2021, and during the investigation carried out in spring 2021, have shown to be stable within 0.6% which is consistent considering that the portable ICT was moved and reinstalled in April 2021. The stability of the ICTs ratio throughout the investigation carried out in spring 2021 was 0.2%.

2.4.2. In water measurement

The following section will present the result of the beam monitoring in water carried out using the diamond detector prototype B1. The procedure for each set-up was the following: the water tank SSD was measured using a laser based distant measure device (± 3.0 mm, Bosch, Gerlingen Germany) and adjusted using the motorized translation table, shown in Figure 3. Once the SSD was as desired, the aluminum scattering plate was installed on the linac exit window flange for the set-up SSD9-02. The diamond detector prototype was installed and positioned in the water tank and moved in the X and Y direction (orthogonal to the beam, as shown in Figure 7) to a fixed position marked by the laser system installed in the experimental room. For the positioning in the Z direction, the depth, the outer surface of the detector was placed against the inner surface of the water tank polycarbonate window. The detector's depth is set to 10.31 mm which is equivalent to the sum of the water equivalent thickness of the phantom window, 7.76 mm × 1.2, and the distance of the diamond's reference point from its outer surface, 1 mm. A depth dose curve and an initial horizontal and vertical profile at z_{ref} were measured with the linac ES setting of 2 mm. The diamond was recentred accordingly and a second profile was taken for validation. For ES setting of 0.5 mm and between 2 to 10 mm by step of 1 mm, hundreds beam pulses were recorded at z_{ref}. The beam profile in both directions were taken for the ES position 6 mm and 10 mm to evaluate the change in beam size and beam centre position due to ES position.

For the set-up 70 cm, the z_{ref} was evaluated, on average, at a depth of 45.8 mm with a standard deviation of 0.1 mm, consistent within less than a millimetre with the Monte Carlo simulations. The measured z_{ref} for the set-up at SS90-02 was 45.4 mm with a standard deviation of 0.05 mm, also consistent with the simulation within one millimetre. The Monte Carlo simulation predicted a difference of 0.3 mm between the reference depth for both set-ups which is very close to the measured one. The largest deviation of the z_{ref} measured was 0.3 mm, therefore, depth positioning uncertainty is considered nonsignificant for UHPDR electron beam. For consistency in the measurement, the z_{ref} was kept at 46.5 mm for both set-ups, the value obtained by Monte Carlo simulation.

The result of the beam monitoring, profile size and centre position, is presented in Table 4. The first line is the beam centre evaluated when the diamond was positioned following the room laser system. The beam centre position in the second line in table 4 is relative to the reference beam which is the beam when the ES are positioned at 2 mm. These values are evaluated once the coordinates of the centre of the beam have been reinitiated following the measurement in the first line. The number in brackets indicated the standard deviation measured during the 6 weeks of this investigation.

Table 5: The results of the monitoring of the beam profile and position in water with the diamond detector B1 for the investigation in spring 2021.

		SSD70-00		SSD90-02	
	ES position	Horizontal	Vertical	Horizontal	Vertical
Beam center position, relative to room laser (*mm*)	2	-2.0(3)	-1.9(3) -0.6(4)	-2.8(3)	-2.1(6) -0.5(4)
Beam center position, relative to reference beam (*mm*)	2	0.1(1)	0.0(1)	0.2(2)	0.0(4)
	6	0.0(1)	0.0(1)	0.2(3)	0.1(3)
	10	-1.0(4)	0.1(1)	-0.9(5)	0.1(1)
FWHM (*mm*)	2	80.3(2)	80.4(2)	208.6(3)	208.3(3)
	6	81.8(2)	81.5(2)	209.3(5)	208.8(4)
	10	83.3(2)	82.6(2)	210.2(4)	209.4(5)
Flatness over 3 cm Ø (%)	2	90.4(1)	90.4(1)	98.49(4)	98.49(4)
	6	90.9(1)	90.8(1)	98.50(4)	98.50(5)
	10	91.3(1)	91.2(1)	98.51(4)	98.50(4)

As shown in first line of Table 5, the beam centre evaluated when the diamond is centred with the laser system is consistent between the two set-ups. There are two values indicated for the vertical position since the laser has been repositioned during the investigation. This has been done since the two lasers used for vertical alignment were slightly off from each other and one was not focused on the water tank. The beam centre while ES are at position 6 mm and 10 mm, relative to position 2 mm, is as it was expected from the in-vacuum beam measurement. The beam centre for ES position 6 mm is unchanged, but a 1 mm difference is observed for the ES position 10 mm.

The measurement of the beam sizes is consistent with the measurement done in winter 2021, shown in subsection 2.3. The beam size in water for the ES position 2 mm and 6 mm agree within 0.5 mm. However, the measured beam size at an ES position of 10 mm is slightly larger by 1 mm, 83.3 mm compared to 82.1 mm, while the beam size in-vacuum is slightly larger for the measurement carried out in winter 2021 compared to the investigation carried out in spring 2021 as shown in Figure 12. In the case of the measured vertical beam, due to the scattering in water, although the beam size remains stable at the linac exit window, the vertical profile in water slightly changes as well. The change in beam size is consistent for both set-ups studied.

The ratio of the diamond prototype signal measurement at z_{ref} for an ES setting of 2 mm for both reference beams was monitored. The ratio was measured to be 0.139(2) and from Monte Carlo, a value of 0.145 was expected. The 5% difference could be explained by the difference in the beam size in water at z_{ref} simulated compared to the one measured. The beam FWHM calculated by Monte Carlo is about 2 mm larger than measured for the set-up SSD70-00. This difference is not observed for set-up SSD90-02 as the beam size considerably wider, FWHM of 208 mm, than the set-up SSD70-00, FWHM of 82 mm. As shown in Table 4, a change in the FWHM of about 2 mm for the set-up SSD70-00 would impact the dose at the centre by about 5%.

As mentioned in the presentation of the PTB's equipment for UHPDR electron beam, the water tank is equipped with two fix holders on which thimble ion chambers CC13 (IBA Dosimetry, Schwarzenbruck, Germany) are mounted, shown in Figure 3. The thimble chambers are removed every evening out of the water to avoid any possible water infiltration due to a long

water immersion. The centre of the ion chambers are at a depth of 38.2 mm in water, 8.5 mm higher than the beam centre and 75 mm laterally away from the beam centre. The ratio of the thimble chamber raw signal was monitored during measurement. The ion chambers have been positioned with the same precision and although no other monitoring system indicates a significant change in the beam, the average ratio measured can vary up to 40% from day-to-day. The ratio of the thimble chambers signal changes by about 10 to 15% with the dose-per-pulse due to the beam size and central position for the set-up SS70-00 and between 1 to 5% for the set-up SSD90-02. From these measurements, it was concluded that in water, but out of beam, monitoring using ion chambers is not reliable.

2.5. Absolute dosimetry

The absolute dose measurement in the UHPDR electron beams at PTB is achieved through alanine dosimetry (secondary standard). Alanine is an amino acid that once exposed to ionizing radiation, stable free radicals are created proportionally to the total absorbed dose. The free radicals can be detected using electron spin resonance (ESR) spectroscopy. The absolute dose to water measurement from alanine is used to calibrate the fix in-flange ICT, illustrated in Figure 1.

The alanine used at PTB are white cylindrical pellets made of 90.9% Amino acid L-alpha alanine in a 9.1% paraffin wax binder (Harwell, UK). The pellet mass is 60(2) mg with a diameter of 4.8(1) mm and a height of 2.8(1) mm, density of 1.184 $g \cdot cm^{-3}$. A total of eight pellets are piled in the vertical direction in a sealed PMMA sleeve which mimics a farmer ion chamber shape (see Farmer design, in figure 3 of [8]). As alanine is known to have a dose response temperature dependence, the water temperature in the phantom is recorded using a PT100 platinum resistance temperature sensor during the irradiation, shown in Figure 3. To ensure temperature equilibrium through the alanine pellets, the PMMA-alanine assembly is immersed for 10 minutes before being exposed to about 15 Gy. A correction factor is applied to measurements which account for the water temperature as shown in the following equation:

$$k_T = 1 - c_T \cdot (T - T_0),$$

where c_T is a constant equal to $1.9(2)10^{-3}$K, T0 is the reference temperature, 293.15 K and T is the water temperature during measurement.

The concentration of the alanine free radicals is read by the Bruker EMX 1327 ESR spectrometer (Bruker, MA, United States) ESR system at PTB. The alanine dose-response is calibrated through ^{60}Co alanine absorbed dose measurement traceable to the water calorimeter PTB's primary standard [9]. The uncertainty of the alanine absorbed dose measurement in ^{60}Co is between 0.4-0.6% [8]. The details about alanine dosimetry in electron beam and uncertainty can be found in the following publications [8], [10]–[12]. The alanine dose-response in an electron beam is different than in photon beam calibration ^{60}Co beam. Therefore, the alanine dose measurement is corrected using the beam quality correction factor, $k_{Al.,E}$, which has a consensus value of 1.014(5) (McEwen et al 2020).

To determine the absorbed dose to water from alanine, the average dose measurement from the eight pellets is used. For the ^{60}Co beam, as the beam is uniform over the detector, the average is equal to the absorbed dose in the center of the beam and the standard deviation between pellets is used to estimated type A uncertainty. For the beams of the set-ups selected as the reference for UHPDR, i.e., SSD70-00 and SSD90-02, the beam profile is not uniform through length of the detector (i.e. the pile of eight pellets). Therefore, the average of all measured pellets is an underestimation of the absorbed dose at the reference point. The relative response of each pellet is determined and a correction factor, equivalent to the maximum

found, is applied to the average dose calculated. This calculation technique has shown to be equivalent to finding the maxima of a fitted third order polynomials.

2.5.1. Monte Carlo simulation

In addition to the previously mentioned correction factor for beam quality and environmental parameters (i.e. water temperature), the measurement in the PTB UHPDR electron beams require additional correction for beam positioning and non-uniformity (profile). For the vertical direction (y-axis), as the alanine measurement is done over eight pellets, it is possible to directly estimate the positioning correction factor from the dose distribution over the 8 pallets. In the horizontal direction (x-axis), the positioning and non-uniformity was estimated from Monte Carlo simulation. As the beam quality correction factor $k_{Al.,E}$ can be geometry dependent [10], the Monte Carlo simulation was used to evaluate it in the PTB UHPDR electron beams. The correction for beam positioning and non-uniformity were compared to estimation based on the diamond detector measurement presented in section 2.4.2.

To obtain $k_{Al.,E}$, the dose ratio alanine to water in the electron beam is compared to the same ratio in a ^{60}Co beam. The beam model was a 10×10 cm^2 field at 100 cm from a point source with the spectrum calculated by Mora and Rogers [13] available in `EGSnrc`. A water tank of 30×30×30 cm^3 was positioned at 90 cm from the point source and the absorbed dose to water was calculated for a scoring cylindrical volume of 0.1 cm thick by 0.25 cm radius center at a depth of 5 cm. The PTB research accelerator model used was as described in section 2.2 for an energy slits positioning of 2 mm and the beam offset was removed. The set-up simulated from Table 3 are the one that was selected for the UHPDR research; SSD70-00 and SSD90-02. The water scoring volume was a cylindrical volume of 0.1 cm thick center at a depth of 4.65 cm with a 0.10 cm radius. The type A (statistical) uncertainty limit was set to 0.05%, typically 10^{10} particles in ^{60}Co beam and 10^9 particles for the electron beams simulations.

The density correction files have been generated by modifying the pure alanine density correction files provided in the `EGSnrc` tool kit. The nominal density was changed to 1.184 g·cm^{-3} instead of 1.424 g·cm^{-3}. The chemical composition was modified to include the 9.1% paraffin wax binder. The density correction factor was unchanged as the density correction for crystalline alanine should be used [10]. The effect of the density correction on the obtained $k_{Al.,E}$ has been evaluated by comparing the results to the one using the `EGSnrc` provided density correction file.

For the 3 beams, ^{60}Co and both set-up in electron beams, the absorbed-dose to alanine was simulated to be the dose deposited in the eight alanine pellets. The absorbed-dose is then calculated using the same technique used for measurement. The effect of the presence of the PMMA sleeve and the alanine pellets pile on the $k_{Al.,E}$ has evaluated. The effect of the energy slit (ES) positioning used to change the dose-per-pulse, as described in the previous section 2.4.1, on the positioning and beam uniformity correction factor was evaluated for both axes. A fluence conversion factor to estimate the absorbed dose to water in the scoring volume per electron simulated was calculated to be compared with the value obtained by measurement, ICT signal [nC] versus dose deposited [cGy]. The fluence conversion factor was also calculated by GUM using `FLUKA`.

2.5.2. Beam correction factor for PTB UHPDR electron beam

For the PTB UHPDR electron beam using the set-up SSD70-00, the beam quality correction factor $k_{Al.,E}$ obtained by Monte Carlo simulation has been found to be 1.011(1). The value

obtained is therefore 0.25% smaller than the consensus value of 1.014(5) [12]. The obtained value remains in one sigma of the consensus value. The use of the alanine density correction file available in the `EGSnrc` distribution, compared to custom file, was found to reduce the absorbed dose to alanine by -0.63(7)% and -0.55(7)% for both the ^{60}Co and electron beam respectively. Therefore, no significant impact was observed on the obtained $k_{Al.,E}$ value; -0.08(14)%. The use of the PMMA sleeve was found to increase the conversion factor by 0.19(14)%. However, the presence of additional pellets has the opposite effect, therefore, the obtained $k_{Al.,E}$ value when calculated for a single alanine pellet is found to be the same as for full geometry simulation, a difference of 0.03(14)%. The results obtained for the set-up SSD90-02, the results were within all stated uncertainty.

The calculated $k_{Al.,E}$ already include correction factors for volume averaging in the XY direct and depth for a single pellet. However, as shown with the results of the diamond measurement in Table 5, the laser system and the beam centre are not aligned. Therefore, a correction factor for beam position is required in the x direction (horizontal), the vertical direction is corrected by using a correction factor evaluated directly from the eight pellets measurement. For each ES position used during the calibration, a correction factor was simulated and compared to estimated values from measurements with the diamond detector. As the beam set-up SSD90-02 is close to uniformity, the positioning correction factor was found to be negligible. For the SSD70-00 set-up, based on the values presented in Table 5 and Figure 12, it was possible to estimate a correction factor for each ES positioning used. The value estimated from Monte Carlo and measurement were consistent and smaller than 1.003(1).

The measured vertical correction factor (i.e. to correct the dose average of the 8 pellets with regard to the dose at the maximum) from alanine measurement has been compared to Monte Carlo simulation and values estimated from measurements using the diamond detector. For the beam set-up SSD70-00, the correction factor estimated was 1.021(1) from Alanine, 1.019(1) from diamond and 1.017(1) Monte Carlo. For the beam set-up, an SSD90-02, the correction factor estimated was 1.0050(5) from Alanine, 1.0029(2) from diamond and 1.0030(5) Monte Carlo. The profile measured and simulated in water and alanine is shown in Figure 13. As it is shown in the figure, the calculated vertical beam profile correction factors obtained are sensitive to the beam size which would explain the difference between simulation and measurement for the set-up SSD70-00. The correction factor used will remain the one that is extracted from the alanine measurement and a 0.15% type B uncertainty has been added to the total uncertainty budget as shown in the Table 6.

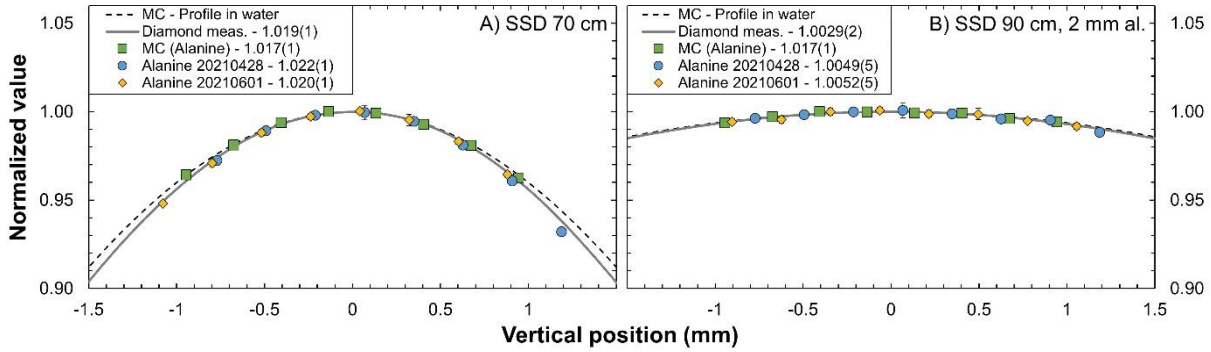

Figure 13: The PTB UHPDR electron beam vertical profile simulated by Monte Carlo on water scoring volume (error bar not shown, ± 0.4%) and in alanine pellets scoring volume, and measured by a diamond detector (error bar not shown, ± 0.2%) and alanine pellets. In A) for the set-up at an SSD70-00 and B) for the set-up at an SSD90-02. The number indicated in the legend is the value estimated for the Y correction factor.

To ease the comparison with the $k_{Al,E}$ consensus value, the alanine detector and source were all centre in the EGS geometry. However, as reported in Table 5, the beam axis is not aligned with the laser system in the room. In the vertical direction (Y axis), any misalignment is implicitly taken into consideration during the analysis of the eight pellets. However, in the horizontal direction, an additional correction factor due to the beam misalignment should be included in the analysis. For the beam set-up SSD70-00, this correction factor was simulated by Monte Carlo. The correction factor was calculated for every ES setting used since the beam center in the horizontal direction is not stable as reported in Table 5. The beam misalignment correction factors were found to be between 1.0021(7) for ES position 2 mm and 1.0000(7) for ES position 10 mm. These simulated values were confirmed by values estimated from the diamond detector measurement. For the beam set-up SSD90-02, the maximum correction was estimated to be 1.0004(2) for diamond detector measurement.

Table 6: Alanine correction factor source and uncertainty budget for the UHPDR electron beam at PTB (k=1).

	Values source	Type A	Type B
^{60}Co dose measurement		0.50 %	
Environmental correction	$k_T = 1–1.9 \cdot 10^{-3} \cdot (T – 293.15)$		0.04 %
$k_{Al,E}$	Monte Carlo calculation; 1.012		0.50 %
Beam shape and position, Y axis	From Alanine measurement		0.15 %
Beam position, X axis	From Monte Carlo simulation		0.10 %
		Combined uncertainty	0.73 %

2.5.3. ICT calibration

As alanine is an integrating offline dosimeter, the evaluation of the absorbed dose to water at the z_{ref} of the PTB UHPDR electron beam is done through a calibration of the fixed ICT [14] illustrated in Figure 1 for a range of dose-per-pulse. The calibration of the ICT has been done in December 2020 with the electron beam set-up SSD70-00. A full calibration, for a range of dose-per-pulse has been repeated twice in May 2021 for both the beam SSD70-00 and SSD90-02, four weeks apart. For each electron beam set-up, the ES positions were changed to vary the dose-per-pulse and the alanine was irradiated for approximately 15 Gy each time. The total number of measurement points was 12, six ES positions for each beam set-ups. The alanine measurement were performed for a single ES position for each electron beam set-up for three weeks between the two full range calibrations.

In the left panel of Figure 14, the results for the calibration with the electron beam set-up at SSD70-00 are presented. A quadratic fitting equation has been selected since the linear fit did not represent the observed measurement trend. This observation was expected due to the beam size change with the ES position which affects the expected linear relationship between the fluence, i.e., the ICT signal, and the absorbed dose-per-pulse in the centre of the beam at z_{ref}. However, the use of a quadratic equation seems to induce a systematic error on the dose estimated for the 2 lowest calibrations points, around 30 nC and 60 nC, as illustrated in Figure 14 B). An additional correction factor for the ICT calibration was estimated from these measurements point.

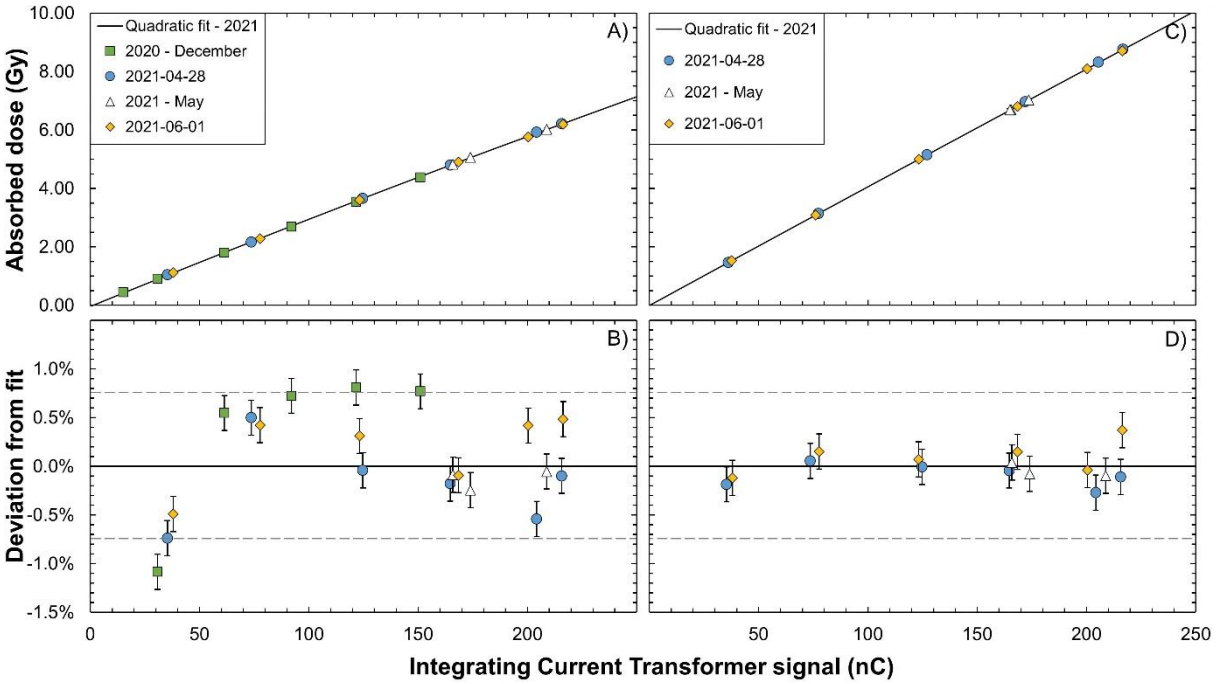

Figure 14: The ICT calibration through alanine absorbed dose to water measurement. The result of the calibration for the electron beam set-up SSD70-00 carried for the investigation in May 2021 and compared to the measurement of December 2020 are presented in A) and B). The quadratic fit has been performed over the measurement in 2021 and the deviation from the fit calculated is presented in B). The results of the calibration for the electron beam set-up SSD90-02 carried for the investigation in spring 2021 are presented in C) and D). The dashed line in B) and D) represent the total uncertainty for alanine measurement while the error bars are the combined uncertainty for the environmental correction and beam shape and position.

The values obtained in spring 2021 for the electron beam set-up SSD70-00 were compared to the calibration that was performed in December 2020. As shown in Figure 14 B), the calibration of December 2020 is within the total uncertainty budget for alanine, however, this included the quality correction $k_{Al,E}$ which affects the value equally. The calibration of December 2020 was performed in slightly different linac parameters set for the RF power and gun power. Some preliminary measurement with the diamond detector prototype has shown that these parameters could impact the signal by up to 1%.

In the right panel of Figure 14, the results for the calibration with the beam set-up at SSD90-02 are presented. A quadratic fit was also used for the calibration curve for uniformity purposes although the change of FWHM of the beam, due to the change of ES, has a smaller impact for this beam set-up.

As mentioned earlier, fluence conversion factor has been calculated using Monte Carlo for the electron beam set-up SSD70-00. From the `FLUKA` simulation, a fluence conversion factor of 2.88(3) cGy/nC was estimated. From the calibration of the ICT by means of alanine absorbed dose to water, this conversion factor was estimated to be 2.92(3) cGy/nC. The difference comes from the deviation of the ICT signal due to the voltage drop on the 40 m long measuring cable. The ICT therefore measures the charge per pulse as being about 1 - 2 % too low.

2.5.4. Diamond detector measurement in calibrated fields

The diamond detector prototype was also used to evaluate the calibration of the ICT for both reference electron beam set-ups. As both beams have similar dose-per-pulse range, the two beams set-ups can be compared for any systematic offset which would be visible by a significant discontinuity between the two measurement ranges. The comparison between the diamond detector signal with the measured absorbed dose to water per pulse is presented in Figure 15. The diamond detector prototype is known to be linear over a large range of dose-per-pulse, but nonlinear behaviour (a loss) is expected in the highest dose range. Therefore, the linear fit presented in the Figure 15 A) and calculated residuum for Figure 15 B) are for a range of dose-per-pulse from 0 to 2 Gy per pulse, which combine values from both electron beam set-ups.

As shown in Figure 15, the diamond detector prototype is showing linear behaviour for signals up to 2×10^{-9}, and for pulse doses from 0.1 to about 3 Gy per pulse. In Figure 15 B), it can be observed that the value obtains for a dose slightly higher than 1 Gy is smaller than the linear fit by 0.5(1)%. This data point is the lowest dose-per-pulse for the set-up SSD70-00. Although this observation is systematic, remains in the total uncertainty budget of alanine.

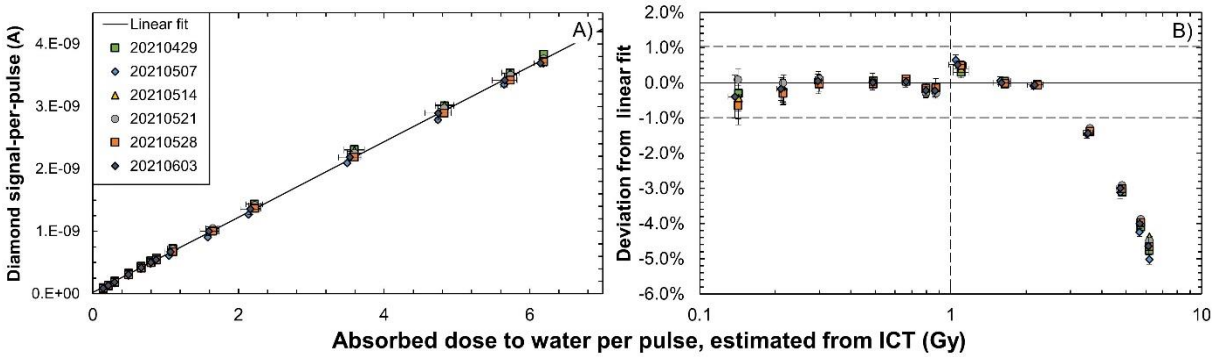

Figure 15: Diamond detector prototype measurement compared to the estimated absorbed dose to water from ICT calibration in A). The values presented are the average for a week of measurement and the error bar represent the standard deviation observed. The linear fit is done for a range from 0 to 2 Gy per pulse for each week separately. The deviation from the linear fit is presented in B) and the horizontal dash line is the total uncertainty budget for Alanine measurement and the vertical one represents the delimitation between both electron beams set-up.

3. METAS - UHPDR reference beam

This chapter will focus on the reference UHPDR electron beam at the electron accelerator at METAS. First, it will cover information about the accelerator hardware and the available equipment. Thereafter, the beam characteristics based on Monte Carlo simulations (done by GUM using `FLUKA`) will be presented together with experimental results.

At METAS, the goal is to characterize the Fricke chemical dosimetry as a possible primary dosimetry technique in a high dose rate electron beam. The chemical yield for Fricke dosimetry is expected to be independent of the electron energy up to 15 MeV [15]. Since the maximum dose rate achievable is rising with electron beam energy, a beam energy of 15 MeV was selected for the MEATS's UHPDR reference electron beams.

3.1. Irradiation Facility

3.1.1. Microtron accelerator

At METAS, a 22 MeV microtron accelerator from Scanditronix (Vislanda, Sweden), shown in **Error! Reference source not found.** A), combine with a conventional clinical treatment head is used to generate clinical electron beams, see **Error! Reference source not found.** B). The microtron provides a pulsed primary electron beam in the energy range of 5 to 22 MeV at a pulse repetition frequency between 1 to 200 Hz and a typical pulse width of 3 µs. The nominal pulse current is in the range of 30 to 100 mA and it is reduced by a factor of 30 with a scattering foil inside the microtron (electron flag). The primary electrons are passing through a 0.2 mm aluminium exit window before they are impinging on one of the scattering targets (see Table 7). The target is usually selected according to the desired nominal electron energy and in order to reach the homogeneity over the field size needed for conventional beams. The treatment head is also equipped with flattening filters.

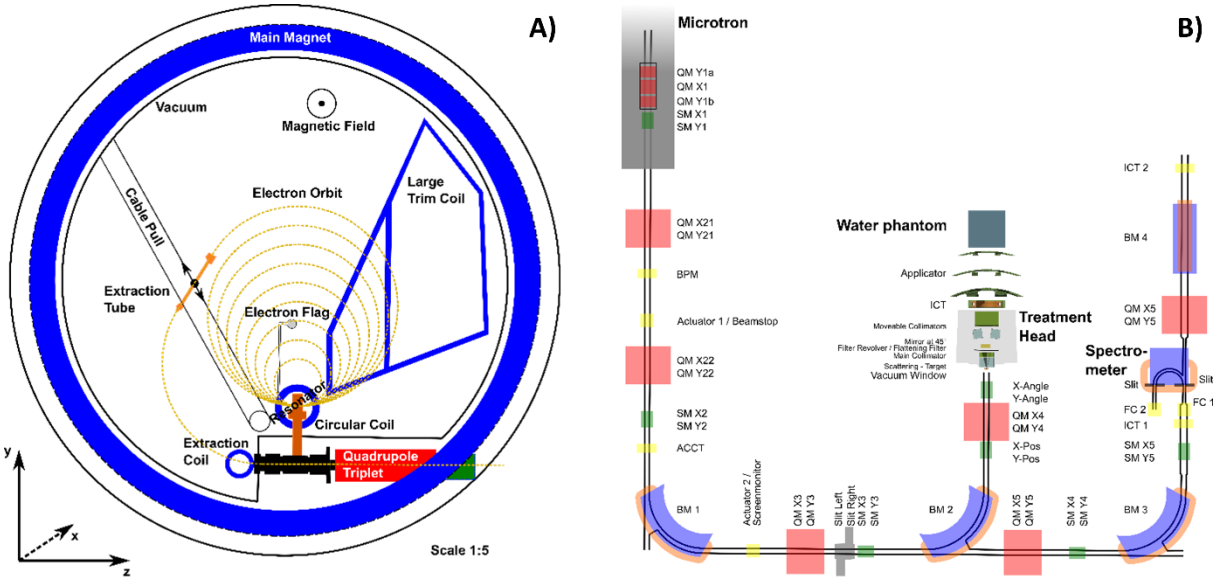

Figure 16: A) Microtron M22 with indicated electron flag. B) Schematic structure of the two M22 accelerator beam lines. The first is equipped with a treatment head designed to deliver conventional therapy beam qualities, the second line is delivering a spatially narrow beam.

A dose rate beyond the conventional range, is achieved by removing the Electron Flag (at turn number 4, see **Error! Reference source not found.** A)) in the microtron[1]. To further increase the dose rate, thinner scattering targets, listed in **Table 7**, and a flattening free filters set-up are used for the UHPDR electron beam.

Table 7: Combination of targets and nominal energies used for the conventional electron beams.

Target number	Conv. used for nominal electron energies (MeV)	Material	Thickness [mm]
5	5, 7.5, 9, 10	Brass + Au	0.05 + 0.025
6	6, 12	Au	0.05
7	15	Au	0.10

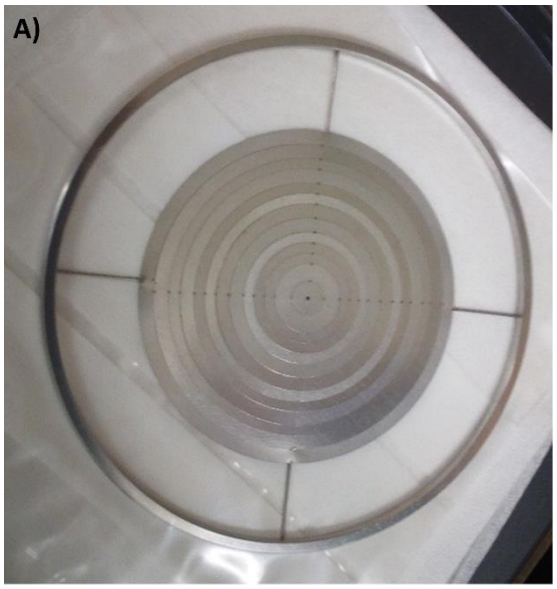

B)

Ø (mm)	Thickness (mm)
5	0.05
10	0.05
13	0.05
16	0.05+0.025
19	0.05+0.025
23	0.05+0.05
27	0.05+0.025
30	0.05+0.025
33	0.05+0.025
37	0.05
40	0.05
44	0.05
48	0.025

Figure 17: A) Flattening filter 2-SC-724/C, conventionally used with a nominal 15 MeV electron beam. It is made of stacked discs of stainless steel as listed in B). The first disc in the list is on the upstream side of the stack.

3.1.2. Equipment

As shown schematically in **Error! Reference source not found.** B), there are two beamlines at METAS facility. The first beamline is equipped with a clinical treatment head, shown in **Figure 18**. The second line is delivering a narrow beam, 3 mm FWHM. This beamline it is equipped with a magnetic spectrometer and a Faraday cup. Both beamlines are equipped with an Integrating Current Transformer (ICT).

Most measurements are performed within a Wellhöfer (Würzburg, Germany) WP700 PMMA water phantom positioned in front of the treatment head. Its inner dimensions are 582×555×615 mm^3 (width (X) × water height (Y) × depth (Z) in beam direction). All PMMA walls, including the bottom, are 10 mm thick, except the front wall which is 35 mm thick. A 2.6 mm thick and 400 mm wide polystyrene plate is glued from the inside of a 160×160 mm^2

[1] This microtron accelerator is designed to deliver clinical electron and photon beams. To achieve the electron beam intensities required, the fluence of primary electrons needs to be significantly lower for conventional electron beams than for photon beams. The electron flag is installed to provide this reduction of primary electrons.

aperture with rounded corners centered on the front wall. The origin of measurement for the water depth is on the outer surface of this entrance window [16].

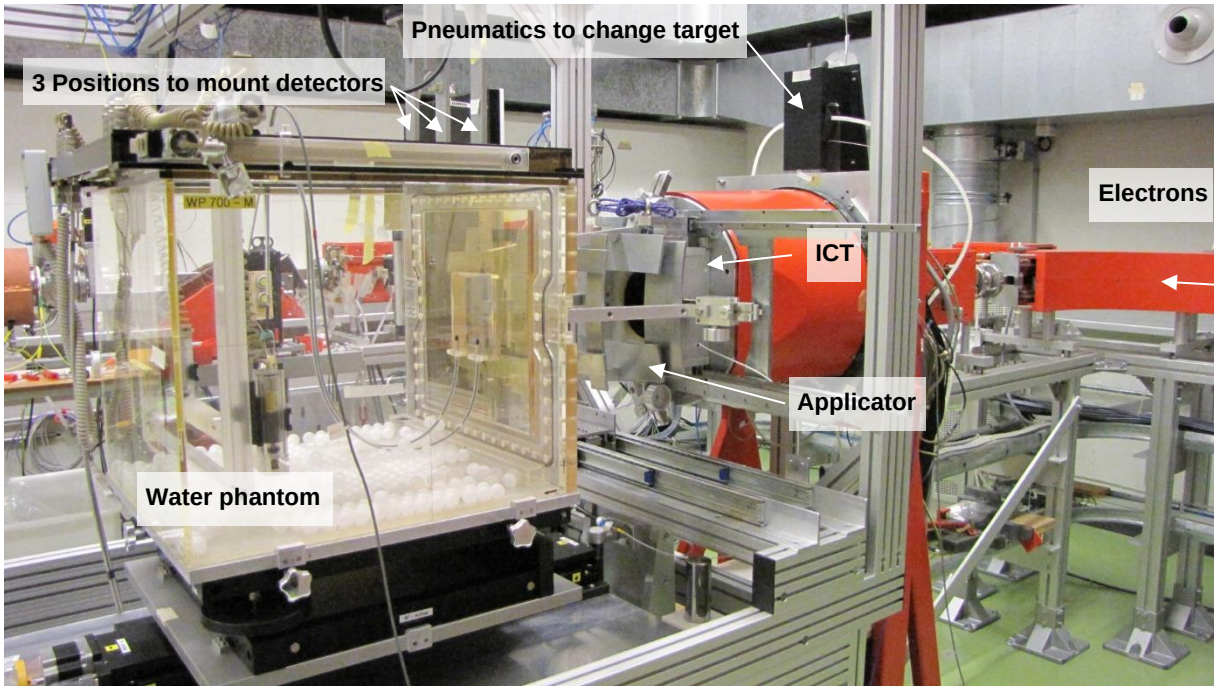

Figure 18: Wellhöfer WP700 phantom, applicator, ICT and treatment head. The water phantom is only filled with water during measurements. The plastic balls are used to prevent water evaporation and thereby minimizing evaporative cooling.

Since the monitor chambers (Type: IC10), installed at the inner surface of the water phantom front wall, are highly saturated during UHPDR measurements, the normalization is based on the ICT measurement between treatment head and applicator. As illustrated in Figure 18, there are three positions to simultaneously mount detectors. They are 12 cm apart, each post is individually adjustable, and the position centred in the beam can be selected remotely. The absolute dosimetry has been done by means of Fricke and Alanine dosimetry. For relative dosimetry, Advanced Markus (PTW, Freiburg, Germany) ion chambers are used.

For Fricke dosimetry, the chemical solution as well as the photometric analysis is done at the METAS facility. A bag made of 50 µm thick polyethylene foil (see **Error! Reference source not found.**, left) is filled with Fricke chemical solution to irradiate with UHPDR pulses. The dimension of the Fricke solution is about 30×45×3 mm^3 (width×height×thickness). The bag is then put into a PMMA holder whose front and back plate are 0.8 mm thick, illustrated in **Error! Reference source not found.**, C). The bottom of the Fricke volume is aligned with the lower edge of the holder. The latter is hanging in the water phantom in such a way that the beam axis passes 25 mm above the lower edge and the middle of the 3 mm thick Fricke volume centre is located at the water depth z_{ref}.

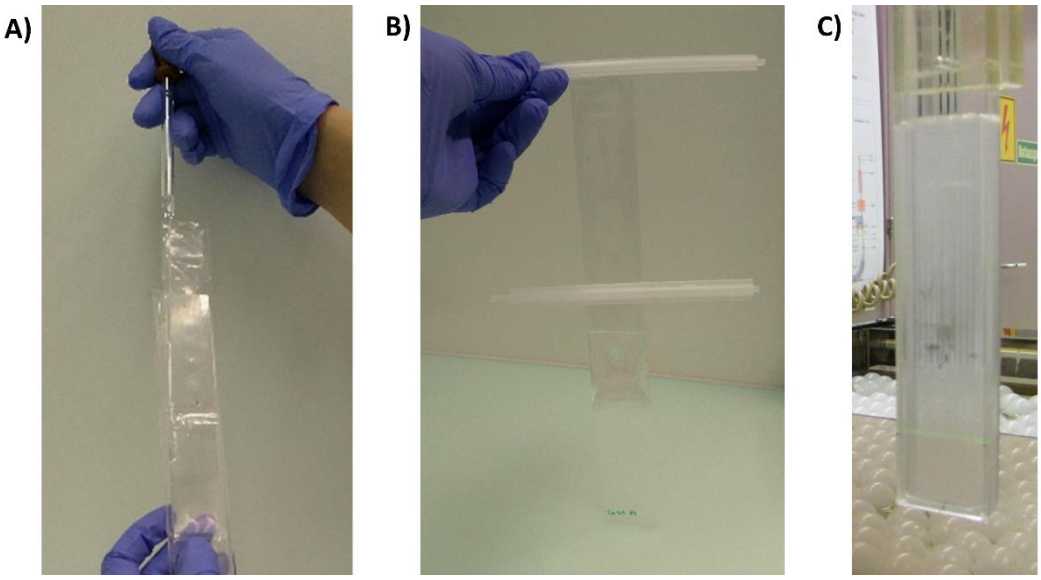

Figure 19: A) Fricke solution is first filled into LD-PE bags. The bag is closed by two clips illustrated in B) and can then by placed into the C) PMMA holder in front of the treatment head (depicted empty).

For Alanine measurements, PTB provided sealed Alanine packages (in PE foils) of four pellets with a size of 5.14×10.85×5.14 mm^3 (width×height×thickness). They were centered in the beam at z_{ref}. The Alanine pellets are positioned using adhesive tape in a hole of a PMMA holder (see **Figure 20**). After irradiation, they were sent back and analyzed by PTB.

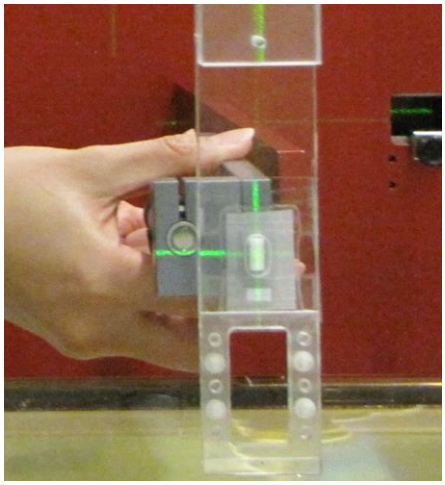

Figure 20: Aligning the Alanine in front of the treatment head.

Further, an Advanced Markus chamber (SN: 2176, or temporary 1185) is in use for UHPDR measurements. During comparison measurements of Fricke, Alanine and Advanced Markus, coefficients for a saturation correction according to the Petersson-type formula (see eq. 2) [17] were determined based on the measured dose per pulse (DPP) of Alanine.

$$k_s = \left(1 + \left(\frac{DPP\ [mGy]}{U\ [V]}\right)^{\alpha}\right)^{\beta}, \qquad \text{Eq. 2}$$

where U is the polarizing voltage across the chamber, and α and β are fitting constants.

For rough relative measurements, Gafchromic film (EBT3) is analysed using an Epson V850pro film flatbed scanner in 48 bit colour mode, scanning with a resolution of 96 dpi. The calibration is based on Co-60 irradiations. The maximal 4 cm wide film strips are irradiated with 3-4Gy. Only the red channel is analysed according to [18].

3.2. Beam characteristic

In this section, the in-beamline characterisation of the electron beam shape and energy spectrum will be presented. This characterisation, together with detailed geometrical information of the METAS accelerator equipment were used as starting point for the development FLUKA Monte Carlo model at GUM, which will be described in subsection 3.2.2. The simulated electron beam characteristics in water, together with experimental measurements are presented in subsection 3.2.3.

3.2.1. UHPDR electron beam characteristics in beamline

For the nominal 15 MeV electron beam, the mean electron energy was measured to be 14.863 MeV with a 25 keV FWHM (Gaussian distribution). The in-vacuum beam has a spatial Gaussian distribution with a 3 mm FWHM [16].

3.2.2. Beam set-up investigated with Monte Carlo (GUM)

The FLUKA 2011-3.0 is a software toolkit to perform Monte Carlo simulation of particle and nuclei transport and interaction with matter. The advanced interface Flair 3.0-1 was used to calculate the absorbed dose in water phantom for the METAS reference 15 MeV electron beam. The electron beam source was simulated as a parallel beam (mean electron energy 14.863 MeV) using the BEAM card module. For all beam energies simulated, a Gaussian energy spread was applied with a FWHM of 25 keV. The spatial gaussian spread of the parallel beam was also applied with a FWHM of 3 mm. The Monte Carlo simulations were based on the geometry of the treatment head components in electron mode [16]. These components are the: primary scattering foil, primary collimator, secondary scattering foil, dose monitor chamber, mirror, X and Y jaws and applicator. It was assumed the beam pipe exit window it made of aluminium of 0.2 mm thickness. The foils are made from different materials with different thicknesses depending on the treatment head settings, which are listed in the above table.

Table 8: Beam a parameter description for the METAS reference electron beam simulation with FLUKA.

	Nominal energy (MeV)	Target number	Target thickness and material	Filter	Mirror in the treatment head	Transmission chamber	Collimator
1	15	7	0.1 mm Au	2-SC-724/C	Yes	No	Yes
2	15	5	0.05 mm Brass and 0.025 mm Au	None	Yes	No	Yes
3	15	6	0.05mm Au	None	Yes	No	Yes
4	15	7	0.1 mm Au	None	Yes	No	Yes

The PRECISIO standard defaults set was used to configure the physical transport and interaction parameters of the simulations. The electron and photon, ECUT and PCUT, kinetic cut-off energies were set to 0.521 and 0.01 MeV respectively. No variance reduction techniques were used. The dose distribution was scored using the USRBIN scoring card in a water phantom of 30×30×30 cm^3 positioned at 100 cm from the source. The scoring volumes were voxels of 0.2×0.2×0.2 cm^3. The USRTRACK card was used to determine the fluence energy. To reach higher precision, the number of histories was set to 5×10^8 for each simulation with 5 cycles.

3.2.3. UHPDR electron beam characteristics in water

All simulations, as well as experimental measurements, were done at the SSD of 100 cm. For a conventional 15 MeV electron beam and for the settings leading to the highest dose rate, the percentage depth dose (PDD) curve was measured using an Advance Markus ion chamber (SN: 1185). The correction used for saturation correction (k_{sat}) was previously determined with respect to Alanine absorbed dose measurement to water. The PDDs curve measured and simulated are in good agreement and indicate a target dependent beam quality index, R_{50}, as illustrated in Figure 21.

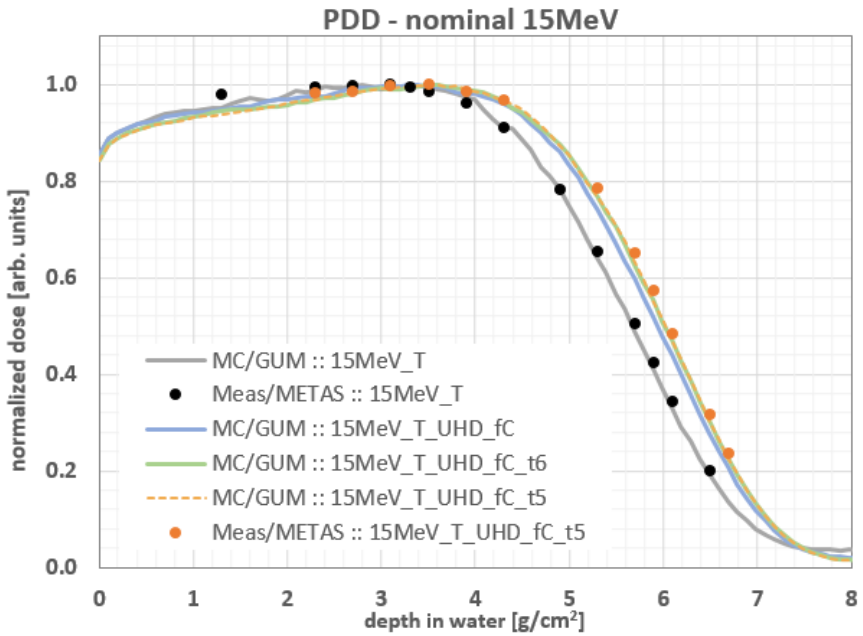

Figure 21: Percentage depth dose curves for conv. (black) and UHPDR machine settings. Solid line: Monte Carlo simulation, dots: measurements done with an Advanced Markus chamber.

From the simulated PDD, the half-value depth in water, R_{50}, was determined and subsequently the reference depth z_{ref}, as defined in Eq. 1, was derived. For each optimized beam setting, the corresponding reference depth, together with typically measured dose per pulse and the dose rate in pulse, are listed in Table 9.

Table 9: Compilation of settings and typical dose rates regularly reached for 15MeV conventional (top raw) and UHPDR settings.

Nom. El. Energy [MeV]	Mean el. energy [MeV]	El. Flag	Target nr.	Flattening filter	z_{ref} (Monte Carlo) [g/cm²]	Typical dose per pulse (3us) [mGy]	Typical dose rate in pulse [Gy/s]	Label of machine settings
15	14.863	in	7	2-SC-724/C	3.30	3	1.00E+3	15MeV_T
15	14.863	out	7	2-SC-724/C	3.30	100	3.33E+4	15MeV_T_UHD
15	14.863	out	7	-	3.47	250	8.33E+4	15MeV_T_UHD_fC
15	14.863	out	6	-	3.50	400	1.33E+5	15MeV_T_UHD_fC_t6
15	14.863	out	5	-	3.51	870	2.90E+5	15MeV_T_UHD_fC_t5

To reach intermediate dose rates (not listed in Table 9), the accelerator is set up on a higher dose rate and the gun current is increased. This leads to a decrease of about 25% maximum reduction of the dose rate. For different machine settings, lateral dose profiles are shown in Figure 22. For UHPDR settings, the measured profiles by EBT3 film indicate a slightly broader beam profile than expected from Monte Carlo simulations (for the settings of typically 400mGy/Pulse, FWHM is 7% larger, for 870mGy/Pulse 0.2%.). Furthermore, the measured profiles are slightly asymmetrical. However, this might be due to a not well centred electron beam at the target. Work on the improvement of the symmetry is ongoing.

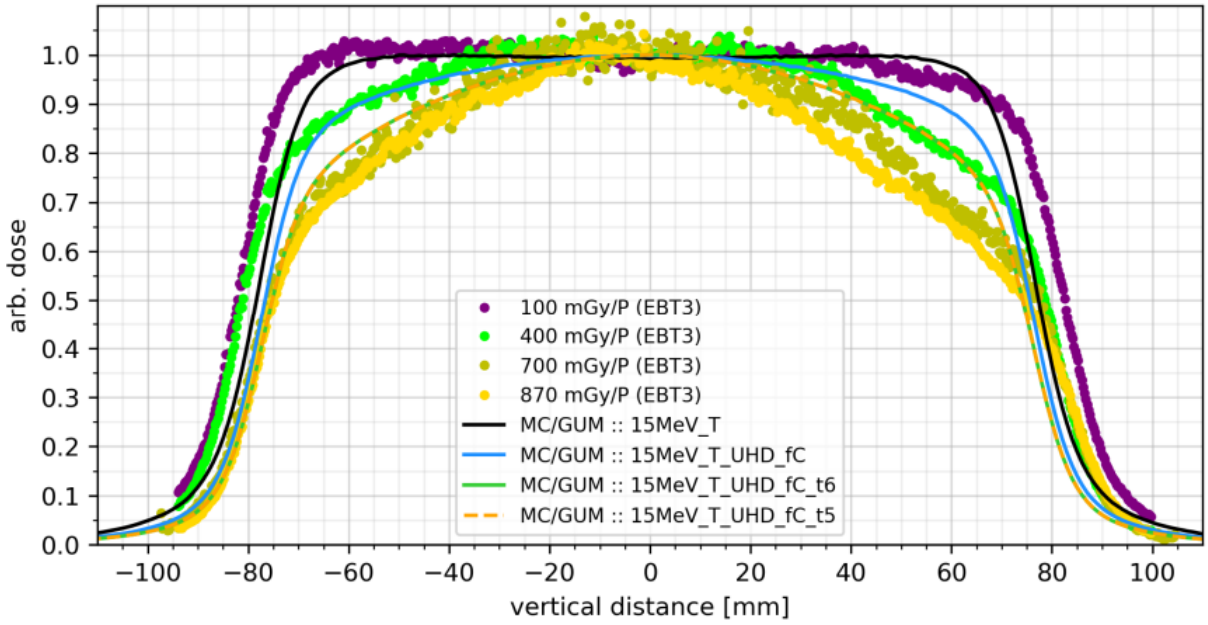

Figure 22: Lateral profiles in vertical direction. Solid lines: Monte Carlo simulations, dots: experimental results measured with gaphchromic film EBT3. For increasing dose rates, the flatness of the lateral profile is significantly decreased.

3.3. Absolute dosimetry

Absolute dosimetry is done through Fricke dosimetry as briefly explain in section 3.1.2. The establishment of primary standard Fricke dosimetry for FLASH electron RT at METAS is the Activity 1.2.2 and will be reported in Deliverable 3 along with the Establishment of PTB's water calorimeter primary standard for FLASH electron RT.

4. References

[1] A. Schüller, S. Pojtinger, M. Meier, C. Makowski, and R. P. Kapsch, “The metrological electron accelerator facility (MELAF) for research in dosimetry for radiotherapy,” in *IFMBE Proceedings*, 2019, vol. 68, no. 3, pp. 589–593, doi: 10.1007/978-981-10-9023-3_109.

[2] A. Schüller, J. Illemann, F. Renner, C. Makowski, and R. P. Kapsch, “Traceable charge measurement of the pulses of a 27 MeV electron beam from a linear accelerator,” *J. Instrum.*, vol. 12, no. 3, 2017, doi: 10.1088/1748-0221/12/03/P03003.

[3] I. Kawrakow, D. W. O. Rogers, E. Mainegra-Hing, F. Tessier, R. W. Townson, and B. R. B. Walters, “EGSnrc toolkit for Monte Carlo simulation of ionizing radiation transport.” 2000.

[4] G. Battistoni *et al.*, “The FLUKA Code: An Accurate Simulation Tool for Particle Therapy,” *Front. Oncol.*, vol. 0, no. MAY, p. 116, 2016, doi: 10.3389/FONC.2016.00116.

[5] P. R. Almond *et al.*, “AAPM’s TG-51 protocol for clinical reference dosimetry of high-energy photon and electron beams.,” *Med. Phys.*, vol. 26, no. 9, pp. 1847–1870, 1999.

[6] International Atomic Energy Agency, “Absorbed dose determination in external beam radiotherapy: an international code of practice for dosimetry based on standards of absorbed dose to water.,” *Tech. Rep. TRS-398, IAEA, Vienna;*, 2000.

[7] R. L. Carver, K. R. Hogstrom, M. J. Price, J. D. LeBlanc, and G. M. Pitcher, “Real-time simulator for designing electron dual scattering foil systems,” *J. Appl. Clin. Med. Phys.*, vol. 15, no. 6, pp. 323–342, Nov. 2014, doi: 10.1120/jacmp.v15i6.4849.

[8] M. Anton, “Uncertainties in alanine/ESR dosimetry at the Physikalisch-Technische Bundesanstalt,” *Phys. Med. Biol.*, vol. 51, no. 21, pp. 5419–5440, Nov. 2006, doi: 10.1088/0031-9155/51/21/003.

[9] A. Krauss, “The PTB water calorimeter for the absolute determination of absorbed dose to water in 60Co radiation,” *Metrologia*, vol. 43, no. 3, pp. 259–272, Jun. 2006, doi: 10.1088/0026-1394/43/3/008.

[10] M. Anton, R. P. Kapsch, A. Krauss, P. Von Voigts-Rhetz, K. Zink, and M. McEwen, “Difference in the relative response of the alanine dosimeter to megavoltage x-ray and electron beams,” *Phys. Med. Biol.*, vol. 58, no. 10, pp. 3259–3282, May 2013, doi: 10.1088/0031-9155/58/10/3259.

[11] S. Vörös, M. Anton, and B. Boillat, “Relative response of alanine dosemeters for high-energy electrons determined using a Fricke primary standard,” *Phys. Med. Biol.*, vol. 57, no. 5, pp. 1413–1432, Mar. 2012, doi: 10.1088/0031-9155/57/5/1413.

[12] M. McEwen, A. Miller, I. Pazos, and P. Sharpe, “Determination of a consensus scaling factor to convert a Co-60-based alanine dose reading to yield the dose delivered in a high energy electron beam,” *Radiat. Phys. Chem.*, vol. 171, p. 108673, Jun. 2020, doi: 10.1016/j.radphyschem.2019.108673.

[13] G. M. Mora, A. Maio, U. De Lisboa, A. Prof, and G. Pinto, “Monte Carlo simulation of a typical Co therapy source,” *Med. Phys.*, vol. 26, no. 11, pp. 2494–2502, 1999.

[14] A. Schüller, J. Illemann, F. Renner, C. Makowski, and R. P. Kapsch, “Traceable charge measurement of the pulses of a 27 MeV electron beam from a linear accelerator,” *Journal of Instrumentation*, vol. 12, no. 3. Institute of Physics Publishing, p. P03003, Mar. 03, 2017, doi: 10.1088/1748-0221/12/03/P03003.

[15] A. PR, “The physical measurements of electron beams from 6 to 18 Mev: absorbed dose and energy calibration,” *Phys. Med. Biol.*, vol. 12, no. 1, pp. 13–24, 1967, doi: 10.1088/0031-9155/12/1/302.

[16] S. Vörös, “Results of the Monte Carlo simulation project.” METAS, 2010.

[17] K. Petersson *et al.*, “High dose-per-pulse electron beam dosimetry - A model to correct

for the ion recombination in the Advanced Markus ionization chamber," *Med. Phys.*, vol. 44, no. 3, pp. 1157–1167, Mar. 2017, doi: 10.1002/mp.12111.

[18] Maud Jaccard *et al.*, "High dose-per-pulse electron beam dosimetry: Usability and dose rate independence of EBT3 Gafchromic films" *Medical Physics*, vol. 44, issue 2, pp. 725-735, 2017

Table 10: Expected beam characteristic of the simulated set-up for the reference electron UHPDR beam at PTB facility. These beams have been simulated using `EGSnrc cavity` application. The expected dose range have been calculated based on initial absolute dosimetry of the beam with an SSD of 70 cm using Alanine. The number in bracket is de difference between the measured and simulated value.

		SSD50-00	SSD50-00c	SSD50-01c	SSD50-02c	SSD70-00	SSD90-00	SSD90-02
SSD (cm)		50	50	50	50	70	90	90
		-	PVC	PVC 1 mm Al.	PVC, 1 mm Al. and FF	-	-	2 mm Al.
	Dose range (Gy per pulse)	[1.7, 12]	[2.0, 15]	[1.0, 7.3]	[0.65, 4.9]	[0.90, 6.7]	[0.56, 4.2]	[0.13, 1.0]
	R_{50} (cm)	74.5(-0.9)	70.6(-0.4)	69.8(-0.9)	66.8	79.2(-0.5)	81.2(-1.0)	78.6(-0.8)
	z_{ref} (cm)	43.7(-0.5)	41.4(-0.2)	40.9(-0.5)	39.1	46.5(-0.3)	47.7(-0.6)	46.2(-0.5)
	R_{95} (cm)	32.2(0.3)	33.6(0.4)	34.2(0.7)	30.4	42.0(1.1)	49.9(0.7)	55.4(-0.4)
	Flatness at depth z_{ref}	17(0.9) %	14(1.7) %	8.0(-0.1) %	4%	9.3(0.4) %	5.9(0.9) %	1.5(-0.05) %
	Flatness at depth R_{95}	18(0.7) %	13(0.9) %	2%	2%	9.5(0.4) %	5.6(0.1) %	2%
	FWHM at z_{ref}	60(-1)	49(-2)	53(-2)	54	82(-2)	103(-2)	208(1)
	FWHM at iso. 95%	57(-2)	50(-2)	53	54	81(-2)	104(-2)	211
Energy at tank surface (MeV)	Spectral Peak	19.9	19.8	19.5	19.0	19.8	19.8	19.0
	Average	19.7	18.6	17.1	15.6	19.6	19.5	18.4
Energy at z_{ref} (MeV)	Spectral Peak	11.8	12.2	11.6	11.5	11.2	10.9	10.2
	Average	9.2	9.2	8.3	8.0	8.5	8.2	7.6